Environmental Science & Technology

pubs.acs.org/est

Article

Quantifying Proximity, Confinement, and Interventions in Disease Outbreaks: A Decision Support Framework for Air-Transported Pathogens

Tami C. Bond,* Angela Bosco-Lauth, Delphine K. Farmer, Paul W. Francisco, Jeffrey R. Pierce, Kristen M. Fedak, Jay M. Ham, Shantanu H. Jathar, and Sue VandeWoude

Cite This: *Environ. Sci. Technol.* 2021, 55, 2890−2898

Read Online

ACCESS | Metrics & More | Article Recommendations | Supporting Information

ABSTRACT: The inability to communicate how infectious diseases are transmitted in human environments has triggered avoidance of interactions during the COVID-19 pandemic. We define a metric, Effective ReBreathed Volume (ERBV), that encapsulates how infectious pathogens, including SARS-CoV-2, transport in air. ERBV separates environmental transport from other factors in the chain of infection, allowing quantitative comparisons among situations. Particle size affects transport, removal onto surfaces, and elimination by mitigation measures, so ERBV is presented for a range of exhaled particle diameters: 1, 10, and 100 μm. Pathogen transport depends on both proximity and confinement. If interpersonal distancing of 2 m is maintained, then confinement, not proximity, dominates rebreathing after 10−15 min in enclosed spaces for all but 100 μm particles. We analyze strategies to reduce this confinement effect. Ventilation and filtration reduce person-to-person transport of 1 μm particles ($ERBV_1$) by 13−85% in residential and office situations. Deposition to surfaces competes with intentional removal for 10 and 100 μm particles, so the same interventions reduce $ERBV_{10}$ by only 3−50%, and $ERBV_{100}$ is unaffected. Prior knowledge of size-dependent ERBV would help identify transmission modes and effective interventions. This framework supports mitigation decisions in emerging situations, even before other infectious parameters are known.

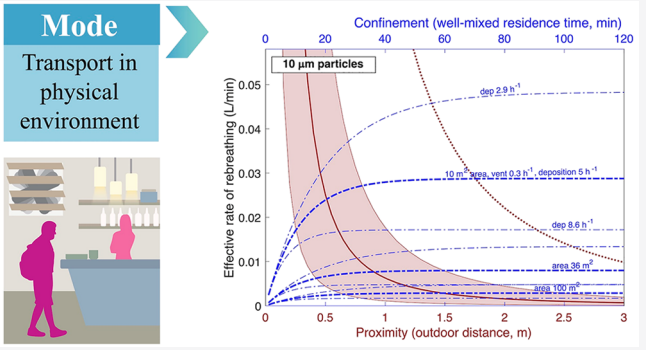

KEYWORDS: *aerosol, indoor air, airborne disease, ventilation, COVID-19*

INTRODUCTION

The spread of the SARS-CoV-2 virus has created a public health crisis and widespread economic disruption.[1] Key factors in the extent of this crisis are (i) the severity of the disease, COVID-19, so avoidance is preferred over illness; (ii) transmission by asymptomatic or presymptomatic individuals;[2,3] and (iii) the novelty of the disease, so that decisions must occur before scientific investigations are definitive. Although this situation is unprecedented in the past century, pandemics have occurred throughout human history. An event like COVID-19 was predicted before its onset[4] and is likely to occur again with different infection dynamics.[5,6]

Figure 1 illustrates the chain of infection,[7] modified to emphasize the role of person-to-person interactions. After a pathogen has entered the human population, escape from the human reservoir depends on the prevalence and characteristics of disease carriers or emitters. On the receiving end, the likelihood of infection is determined by the host's susceptibility and the dose received. The mode is the method of travel between the pathogen's release and the host. The pathogen's survival characteristics limit viable modes, but the environment modulates the transferred dose. This environment includes the social system that compels intersection between individuals and the physical environment through which the pathogen travels. Uncertainty about physical transmission has led to suspicion about the interactions that underpin the economy. The ability to quantify exposure risks in social interactions more quickly and rigorously would aid decision-making in current and future outbreak situations.

Describing the chain of infection requires expertise in epidemiology, infectious disease, sociology and data science, engineered and natural environments, virology, immunology, and public health. Each field has burgeoned since Riley's pioneering work[8] combined carrier and environmental characteristics into a single equation, yet few metrics distill

Received: November 15, 2020
Revised: January 19, 2021
Accepted: January 19, 2021
Published: February 19, 2021

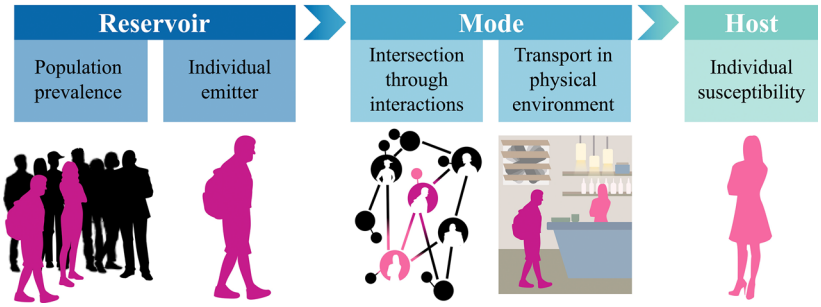

Figure 1. Chain of infection for a disease whose spread depends on human interactions. Figure credit: Mj Riches.

the essential elements of the chain for use in collaboration. The separation of emitter, environment, and host characteristics would allow experts to collaborate more rapidly during an emerging situation. This paper describes a metric to quantify pathogen transport and uses it to compare transmission environments and mitigation measures.

A particular challenge in any emerging situation is uncertainty in the mode of transmission. Public health guidance[9] uses the terms "droplet" and "short-range" for large expiratory particles that transport through air but are lost quickly by falling. A second mode, via small particles that tend to follow airstreams, is termed "airborne", "aerosol", or "long-range". A third mode is called "indirect" when pathogens are transferred through intermediate, contaminated objects, including human skin.[10] Dominant modes of transmission are hotly debated for COVID-19[11,12] and other respiratory infections.[13] Despite the differences in terminology, the dynamics of transport through air govern the first two modes and play a role in the third.

The approach we present does not champion any particular mode but instead acknowledges the importance of particle size in every step of the chain of infection. Particle size and viral content are influenced by where particles originate within the respiratory tract;[14] size affects the depth of penetration into the recipient's lungs and susceptibility.[15] Size dominates particle fate; large particles do not remain suspended as long and are easier to remove because of the relative influences of gravity, drag force, and attachment to surfaces or deposition.

METHODS

Quantifying Person-to-Person Transport. A metric to characterize and communicate person-to-person transport should be understandable by individuals outside the field, able to encapsulate complex situations and incorporate evolving knowledge, generalizable to archetypal building situations, and germane to decision making by comparing alternative interactions. It should not be confounded by differences in human emitters or recipients, which are independent of transport.

We choose *rebreathed volume* (RBV) as a basic metric for this purpose. RBV is the total volume of air exhaled by one person and subsequently inhaled by another. RBV is proportional to the *total* dose that an individual receives; we also use the *rate* of rebreathing to compare different interactions of equal lengths. If a recipient were inhaling directly from the mouth of an emitter, the rebreathing rate would be the human breathing rate of 8 L min^{-1},[16] and over 10 min, RBV would be 80 L. RBV can be calculated from simple models, computational fluid dynamic models, and tracer measurements in both indoor and outdoor situations (SI S.1−S.4).

RBV is similar to other metrics and can be calculated from them (SI S.9), including the Wells−Riley equation for probability of infection,[8] inhalation intake fraction,[16] or rebreathed fraction.[17] However, RBV quantifies the role of the transmission environment, separate from individual characteristics of carriers and hosts. It does not require a quantum generation rate as does the Wells−Riley equation and is independent of the number of participants, unlike intake fraction and rebreathed fraction. RBV quantifies person-to-person sharing of breath during standard conditions and activities. To determine risk of infection for specific activities, occupancies, and diseases, crowding effects and adjustments to breathing rates need to be applied (SI S.9). Some analyses have presented the entire chain of infection for SARS-CoV-2 transmission,[18−20] but they have not isolated the environmental component as is done here.

To communicate transport dynamics of differently sized particles while maintaining simplicity, we define *effective rebreathed volume* (ERBV) as the exhaled volume that contains the same number of particles as the air inhaled by the recipient. If a recipient received 80 L of RBV from an emitter, and 90% of particles with diameter X were lost by settling, then $ERBV_X$ would be 8 L (80 L multiplied by 10% remaining). This physics-based treatment allows objective comparison of transmission modes by accounting for the main difference in particle transport: size-dependent loss.

We choose decadally spaced sizes that cover a biologically relevant range: 1, 10, and 100 μm diameter ($ERBV_1$, $ERBV_{10}$, and $ERBV_{100}$, respectively). Sizes of expiratory particles range from 0.01 to 1000 μm,[21−23] although the largest particles are rarely measured. The 1000 μm particles are excluded because they would travel less than 1 m due to their rapid fall speeds. Particles the size of a bare virion (0.1−0.2 μm) probably do not exist in free air, but in any case they would travel like 1 μm particles because they have similar indoor deposition loss rates (SI). Large expiratory droplets evaporate within a few seconds,[24,25] and a 100 μm droplet would become about 20 μm after losing 99% water content.[26] The transport we present assumes that this transformation has already occurred.

Model Selection. Exhaled volume is treated as a conserved tracer with losses that depend on particle size. All equations for transport of a contaminant in fluids can be used to predict exhaled volume per volume of air. A challenge in developing comparative transport metrics has been the limited literature describing the travel of contaminants within a few meters of a source or emitter, which we call "source-proximate transport." A contribution of this work is therefore a review of modeling approaches to estimate rebreathed volume. The models chosen

https://dx.doi.org/10.1021/acs.est.0c07721
Environ. Sci. Technol. 2021, 55, 2890−2898

are summarized here, and equations and further justification appear in the Supporting Information.

The models ultimately chosen are simple, yet they capture the major factors that affect contaminant transport: distance from emitter, accumulation in confined spaces, dispersion rate, and the influence of other loss rates including mitigation measures. The simulations can therefore be used to compare expected values of rebreathing, even between very different environments such as within and outside of buildings. The chosen models do not rely on specialized inputs such as surface temperatures or roughness or detailed interior geometries. Such requirements would preclude general recommendations and comparisons among environments.

For outdoor interactions, we used a steady-state Gaussian plume equation[27] over a range of atmospheric stability conditions. The Gaussian plume is typically not used to describe transport over short distances, because contaminants travel in irregular packets. However, average concentration values do follow the expected shape, even 2 m from the emitter,[28,29] and the distribution of concentration due to sporadic transport on short time scales can be described probabilistically.[30] We therefore combined the Gaussian-predicted concentrations with an intermittency enhancement[30] as a worst case. SI S.2 provides more details.

For most indoor interactions, we used a well-mixed zone model, which assumes that concentrations are the same throughout each zone. The model was cast in a matrix form[31] to simulate multiple zones, including connections through central air systems (SI S.3). Few reports quantify deviations from the well-mixed zone assumption other than proximity effects. Variations in indoor cooking smoke concentrations can be about a factor of 2 from lowest to highest.[32] Stochastic variations in infection rate from interzonal transport were simulated as about 40%.[31] No evidence suggests that expected values from well-mixed simulations are biased. Stochastic variations do not invalidate comparisons between expected values of rebreathed volume, which are averaged across the entire environment. If those variations are not observable or predictable, they cannot be manipulated to reduce risk, either. The well-mixed zone assumption does not represent displacement ventilation, but deliberate use of this strategy is not widespread. The assumption also ignores stagnation zones, which are much less likely to contain respiring humans than other parts of the room.

Elevated concentrations occur near emitters indoors. We simulated indoor proximity effects with a point-release model,[33] modified to represent a continuous source with dispersion parameters dependent on air-change rates (SI S.4).[34] Simulated concentrations agreed with steady-state, well-mixed values at distances far from the emitter or when dispersion was similar to outdoor values. We assume worst-case rebreathing rates, when the emitter and recipient breathe at the same level. We also interpreted the few available measurements of indoor proximity in terms of ERBV (SI S.4) for comparison. Indoor proximity effects have been simulated with computational fluid dynamic models, but we did not find quantified source or breathing rates that would allow interpretation in terms of rebreathed volume. Computational fluid dynamic studies often simulate particular ventilation, furnishing, or occupancy features; they would be useful to understanding of ERBV by including enough variation to allow generalization.

Selection of Inputs. We identified a range of common floor area and air exchange rates for residential and office situations (SI S.7, S.8), selected for general interest. Residential situations range from small apartments to moderate-sized single-family homes; offices with similar floor areas were chosen for comparability. We used a range of common air exchange rates for each situation (SI S.7, S.8), based on measurements and recommendations from the American Society of Heating, Refrigerating and Air-Conditioning Engineers (ASHRAE).[35,36]

Particle removal by deposition is the reason that ERBV differs among particle sizes and affects effectiveness of mechanical mitigation measures. We use the theoretical model by K. Lai and Nazaroff[37] to provide central values. However, measured deposition is often faster than model predictions,[38] especially for particles smaller than 1 μm and in occupied houses. Uncertainties are taken from observations[39,40] as summarized in SI S.5 and Table S.2.

Mitigation Measures. Mitigation measures focus on reducing the confinement effect indoors and included improving filtration in central air handlers, adding stand-alone air cleaners, staggering occupancy in office situations, and employing exhaust fans and opening windows in residential situations. Removal by filtration occurred at the inlet of the central air system. When natural infiltration dominated air exchange, we accounted for reduced effectiveness of mechanical ventilation.[41]

The importance of each particle size is different for each pathogen and is unknown in an emerging situation, so we present fractional reductions in ERBV for all three particle sizes. Size-dependent filter efficiencies are taken from ASHRAE Standard 52.2-2017[42] with ratings as described Tables S.4 and S.5. Mitigation by ultraviolet disinfection in central air handlers would be comparable to filtration with similar efficiencies. Each mitigation measure was applied to each baseline case, the reduction percentage was calculated, and the entire range of reduction percentages is presented.

Risk Reduction Context. Risk may not be reduced by the same fraction as transmitted dose. Dose−response curves are typically used to infer a change in risk, but quantitative dose−response curves are unknown in an emerging situation and often remain uncertain even for well-studied pathogens. However, dose−response relationships for many viruses have similar features. Human and animal responses typically show a zero risk of infection below a minimum infectious dose, and near-certainty of infection above infectious dose 95% (ID_{95}, also called "saturated"). If the baseline dose is below the minimum infectious value, then mitigation measures are not required. Conversely, if the baseline exceeds ID_{95}, mitigation does not effectively reduce risk without a significant reduction in dose. Between the minimum infectious dose and ID_{95}, dose−response curves often have a sigmoidal shape. At the dose that is likely to infect 50% of susceptible individuals (ID_{50}), infection risk rises approximately linearly with the logarithm of dose. Mitigation measures are effective only when applied over this responsive portion of the curve, and efficacy depends on both the baseline risk relative to ID_{95} and the range, or width, of infectious doses spanned by the sloping portion of the infection curve.

We created two illustrative dose−response curves to demonstrate how the baseline dose and width of the dose−response curve affect expected risk reductions. These two curves have identical values of ID_{50}, but different widths; we

https://dx.doi.org/10.1021/acs.est.0c07721
Environ. Sci. Technol. 2021, 55, 2890−2898

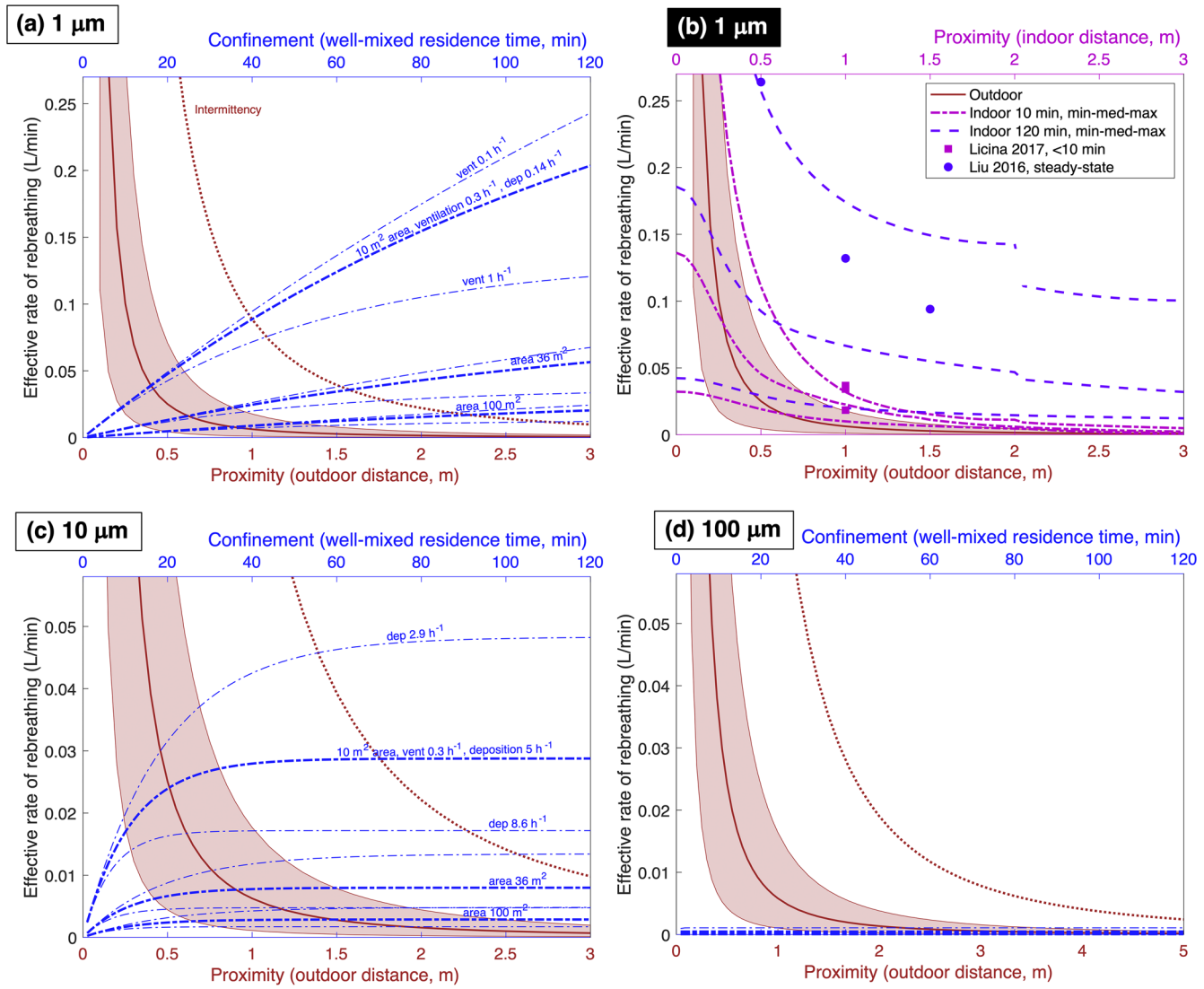

Figure 2. Instantaneous effective rebreathing rate for outdoor (red, with shaded area) and indoor (blue, dashed) interactions for particles of diameter (A) 1 μm; (C) 10 μm; (D) 100 μm. Horizontal axes for proximity (lower) and confinement (upper) axes are not equivalent but appear on the same figure for comparison. Note the difference in vertical axis scales. Rebreathing rates are person-to-person and would increase for more emitters.(B) Comparison of outdoor and indoor proximity for a range of simulated indoor conditions, for 10 and 120 min after emitter entry, and in this figure the horizontal axes are the same.

refer to these as "moderate" and "wide" (Figure S.5). Watanabe et al.[43] summarized studies on SARS-CoV-1, a virus that is similar to SARS-CoV-2. They explored both exponential and beta-Poisson distributions to fit observed risk of infection, recommending the former because the beta-Poisson distribution did not have a statistically better fit. However, the exponential distribution has a fixed width, so we used the beta-Poisson distribution. The "moderate" dose–response curve has a width similar to the synthesized curve of Watanabe.[43] The doses associated with 5% risk and with 95% risk differ by a factor of 100, informally called "2 logs." For the "wide" curve, the distance between 5% risk and 95% risk is a factor of 3100 ("3.5 logs"), similar to estimates by Kitajima et al.[44] for H5N1. Again, we make no assumption that any infectious disease can be represented by these dose–response curves; we use only the curve's shape to connect mitigation measures might reduce risk.

RESULTS AND DISCUSSION

Proximity and Confinement Effects. Figure 2 compares the rate of rebreathing during simple maximum outdoor (red, shaded) and indoor (blue, dashed) interactions for 1, 10, and 100 μm particles. The contrast between the three particle sizes shows the importance of separate consideration. Person-to-person transport of pathogens is greater in close *proximity*, partly because contaminants spread out (disperse) as they travel away from an emitter, and partly because they also fall out (deposit) during that travel. Person-to-person transport is also greater in close *confinement*, where contaminants accumulate when they cannot escape the walls of an enclosure.

Outdoors, concentration decreases with distance from the emitterbecause particles are carried by wind and dispersed by air fluctuations. The proximity effect is especially attributable to dispersion but also deposition for large particles. The gravitational settling that differentiates particles is negligible for 1 μm and 10 μm particles, but some 100 μm particles have fallen out after traveling 2–3 m. Public guidance in 2020

https://dx.doi.org/10.1021/acs.est.0c07721
Environ. Sci. Technol. 2021, 55, 2890–2898

suggests maintaining 2 m separation between individuals, avoiding the highest concentrations. At this distance, the outdoor rebreathing rate is less than 0.01 L min^{-1}, and it would be even lower if the recipient were not directly downwind (Table 1).

Table 1. Person-to-Person Effective Rebreathed Volume for 1 μm Particles ($ERBV_1$) in Common Interactions

	effective rebreathed volume (L)			
interaction	15 min	1 h	4 h	note
outdoors				
directly downwind, 1 m distance	0.02–0.14	0.1–0.58	0.58–0.98	*a–c*
same, 2 m distance	0.005–0.04	0.02–0.14	0.14–0.24	*a–c*
45° from wind dir, 1 m distance	<0.0004	<0.001	<0.006	*a–c*
indoors				
small room, 1 m distance	0.17–0.28	2.7–3.9	12.2–20	*d–f*
same, 2 m distance	0.063–0.071	1.7–2.1	9.1–14	*d–f*
same, well mixed	0.075–0.079	1.0–1.2	8.9–14	*e–g*
communal office, well mixed	0.011–0.012	0.15–0.17	1.2–1.9	*f–h*

[a]ERBV is proportional to interaction time, because there is no confinement effect. [b]Plume model with wind of 2.5 m s^{-1}; urban topography, range of weather conditions. [c]Intermittency increase is not included, because fluctuations average out after 15–20 min. [d]From indoor point-release model, 0.3–0.8 ac h^{-1}. [e]Floor area 36 m^2, height 2.5 m^2, size of small conference room or living room. [f]Assuming emitter and recipient enter simultaneously. [g]From well-mixed zone model, 0.3–0.8 ac h^{-1}. [h]Floor area 200 m^2, height 3 m^2.

Figure 2 also shows rebreathing in well-mixed, enclosed rooms (blue dashed curves), where the confinement effect occurs because exhaled air accumulates rather than dispersing. Within 15 min indoors, the rebreathing rate for 1 and 10 μm particles exceeds that of a 2 m distance outdoors, with more rebreathing in small rooms. An individual who is unwilling to stand within 2 m of a potential emitter outdoors may unwittingly accept the same or greater risk by remaining in a moderate-sized room for 15 min, even at distances greater than 2 m. This is true regardless of variability or uncertainty in model inputs.

Figure 2 demonstrates sensitivities to different assumptions. The rate of rebreathing depends on length of accumulation (upper x-axis throughout Figure 2) and room size (thick blue lines in Figure 2a,c,d). Particles of 100-μm deposit rapidly and do not accrue, so indoor rebreathing is low, consistent with particles classically termed "droplets" (Figure 2d). Ventilation rates reduce rebreathing noticeably for interaction times above about 30 min, as shown for the 1 μm particles in Figure 2a. For these particles, uncertainties due to deposition are relatively small (not shown). Particles of 10 μm diameter deposit more quickly than smaller particles, so indoor $ERBV_{10}$ is lower than $ERBV_1$ (Figure 2c). Nevertheless, rebreathing of 10 μm particles is still important in confined spaces. $ERBV_{10}$ is affected by ventilation (not shown) but is also greatly affected by uncertain deposition rates.

Contaminants disperse quickly indoors,[45] but both proximity and confinement effects occur in enclosed spaces. Figure 2b shows indoor rebreathing rates of 1 μm particles simulated with a point-release model[33,34] for 10 and 120 min after emitter entry. Minimum, median, and maximum values for a range of dispersion rates, emitter positions, and room sizes are presented. The maximum curve is discontinuous because the

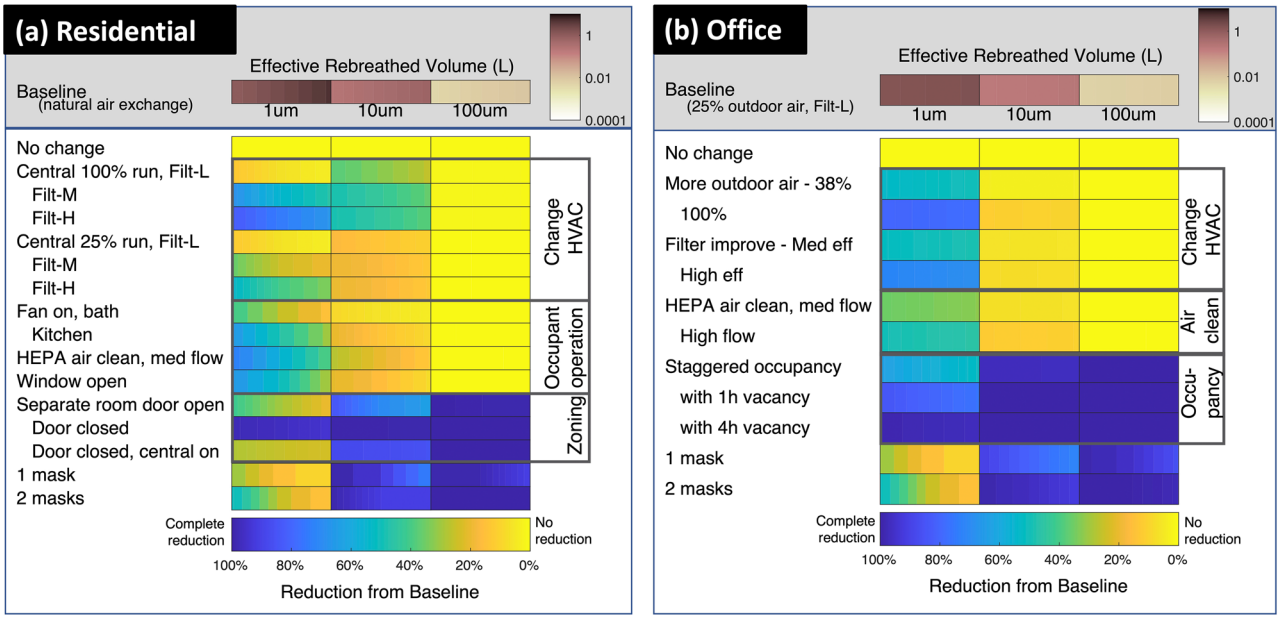

Figure 3. Person-to-person ERBV for 4 h interactions in (A) residential and (B) office settings, along with reductions due to mitigation measures. Horizontal shading in the individual rectangles shows realistic variability in environment and facilities, such as different floor areas (SI). In residential settings, "Central" means operating the central air handlers, common in the United States, continuously (100%) or with a 25% runtime. Most of these systems filter air but do not provide air from outdoors; ventilation is provided with bath and kitchen exhaust fans. The situation differs in office buildings, where continuously operating central air handlers supply cleaned outdoor air as well as filtering recirculated air. "Air cleaner" refers to portable, stand-alone air cleaners with high-efficiency filtration. SI contains additional details, along with figures for 15 min and 1 h interactions.

https://dx.doi.org/10.1021/acs.est.0c07721
Environ. Sci. Technol. 2021, 55, 2890–2898

greatest rebreathing occurs in small rooms of 4 m width, and those simulation results disappear from the summary curve at more than 2 m. Also included are values interpreted from chamber measurements,[46,47] which fall within the simulation range.

After 10 min of residence time, indoor and outdoor proximity effects are similar. An elevated proximity effect, as well as a confinement effect throughout the room, occurs after 2 h. These simulations are simplified; indoor dispersion rates depend on the intensity of turbulence in the room, which in turn is affected by environmental conditions, surface properties, sources of thermal energy, and even the buoyancy around a human body.[47] Regardless of these variations, all simulations demonstrate a sharp decrease in the proximity effect indoors and outdoors within 1−1.5 m. Momentum from breathing, coughing, or sneezing affects travel of particles immediately after emission, and that effect is not modeled here. Except in extreme cases such as violent sneezes, that initial momentum governs transport only within the first 1.5 m.[24] Thus, the 2 m distancing guideline addresses much of the proximity effect, whether it is caused by dispersion or momentum. The purpose of this work is not to quantify the proximity effect in all situations. Rather, we confirm that it exists both outdoors and indoors, that it is greatly reduced at a distance of 2 m, and that the confinement effect is frequently greater than the proximity effect occurring at 2 m, regardless of uncertainties in either one.

Total ERBV is obtained by summing over the recipient's entire residence time. Table 1 summarizes $ERBV_1$ over 15 min, 1 h, and 4 h interactions, which represent a brief face-to-face commercial transaction, a business meeting, and a half-day working session, respectively. The definition of "close contact" from the Centers for Disease Control and Prevention is "within 6 feet for at least 15 min", corresponding to a minimum ERBV of about 0.07 L for any particle size. Regardless of whether the participants are farther apart than 2 m distance, confinement in the two smaller rooms in Figure 2 causes ERBV to exceed the "close-contact" value after about 10−15 min, for both 1 and 10 μm particles.

Effect of Mitigation Measures. Rebreathing can be lessened when the participants remain at a distance to reduce proximity effects. Other solutions are needed to reduce the confinement effect, and those are explored here. Figure 3 summarizes ERBV for a 4 h stay in residential (Figure 3b) and office (Figure 3b) settings.

The upper portion of the figure shows how size-dependent losses affect rebreathing: $ERBV_1$ is 2 orders of magnitude greater than $ERBV_{100}$. This difference does not imply that 1 μm particles have the highest infectivity. If exhaled air contains few or no pathogens of this size, then the efficient transport indicated by high $ERBV_1$ is unimportant. The high value does indicate that even a small release of pathogens in 1 μm particles would be easily transmitted to a recipient. Likewise, the lower value of $ERBV_{10}$ does not indicate unimportance. Particles of 10 μm diameter might be transmitted less efficiently, but this size range could still contain most of the infective particles.

The lower part of each figure shows rebreathed volume reductions by ventilation, filtration, and occupancy or zoning measures. The lowest rows show the effect of cloth or surgical face coverings for comparison, with uncertainty in efficiency shown as a range of shading. For mechanical measures (ventilation and filtration), achievable reductions depend on the fraction of time operating, flow rate compared to room volume, and filtration efficiency. Many common filters remove particles of 10 μm diameter and larger, with efficiencies improving at higher filter ratings; lower rated filters do not remove 1 μm particles.

$ERBV_{100}$ is not noticeably reduced with any ventilation or filtration strategy because these large particles are lost by deposition more quickly than they can be removed mechanically. Offsetting occupancy, wearing face coverings, and separating occupants between rooms—even with doors open—does reduce $ERBV_{100}$.

$ERBV_1$ can be reduced with many ventilation and filtration strategies. Ventilation should bring clean air into the environment, while filtration recirculates and cleans air. Reductions in $ERBV_{10}$ by mechanical measures are intermediate between $ERBV_1$ and $ERBV_{100}$. Some effective mitigation measures would be neglected by assuming that 1 and 10 μm particles are unresponsive to mechanical means like large, 100 μm droplets. In residences (Figure 3a), kitchen range hoods reduce $ERBV_1$ by 30−40% and bath fans, with about half the flow, by only 15−30%. Opening windows reduces $ERBV_1$ by 25−65%, with the wide range caused by differing response to opening size and position. When central-air units operate continuously with medium- or high-rated filters, reductions are 15−55%; lower operating time decreases those benefits. Separating individuals between rooms gives moderate reductions, while closing doors between them is the best protection as long as central air handlers are not operating. Offices have more closely controlled ventilation than do homes, and a narrower range of ERBV and mitigation effectiveness. Increasing the amount of outdoor air supplied and improving the filter both reduce $ERBV_1$, while $ERBV_{10}$ reductions are lower because the baseline already includes some removal of 10-μm particles. Staggered occupancy, in which one person enters after another leaves,[48] reduces $ERBV_1$ similar to medium-rated filtration. Vacancy periods increase the reduction. These findings depend on the assumption of well-mixed spaces and do not include additional management strategies such as personalized or displacement ventilation, which could be investigated further by comparing ERBV values.[49]

Deposition loss rates are a key reason that 1 and 10 μm particles differ in baseline ERBV and also explain differences in the ventilation effectiveness shown in Figure 3. Deposition loss rates for 10 μm particles are similar to or greater than air exchange rates, so total removal is less influenced by intentional ventilation changes. In comparison, removal of 1 μm particles is dominated by air exchange and easily altered by ventilation. A good understanding of indoor deposition rates therefore underlies quantification of ventilation effectiveness, but these loss rates are infrequently measured, and measured deposition is usually faster than theoretical predictions.[50] Further discussion of deposition and its influence on ventilation effectiveness is given in SI S.10.

The difference between $ERBV_1$, $ERBV_{10}$, and $ERBV_{100}$ offers the possibility to determine particle sizes most likely involved in transmission through retrospective analysis. For example, staggered occupancy (one 4 h shift following another) reduces $ERBV_1$ by about 60% but $ERBV_{10}$ by over 99%. In an emerging disease outbreak, the infectious nature of 1 μm versus 10 μm particles might be elucidated by seeking situations in which an index patient infected others in the same shift and did or did

https://dx.doi.org/10.1021/acs.est.0c07721
Environ. Sci. Technol. 2021, 55, 2890−2898

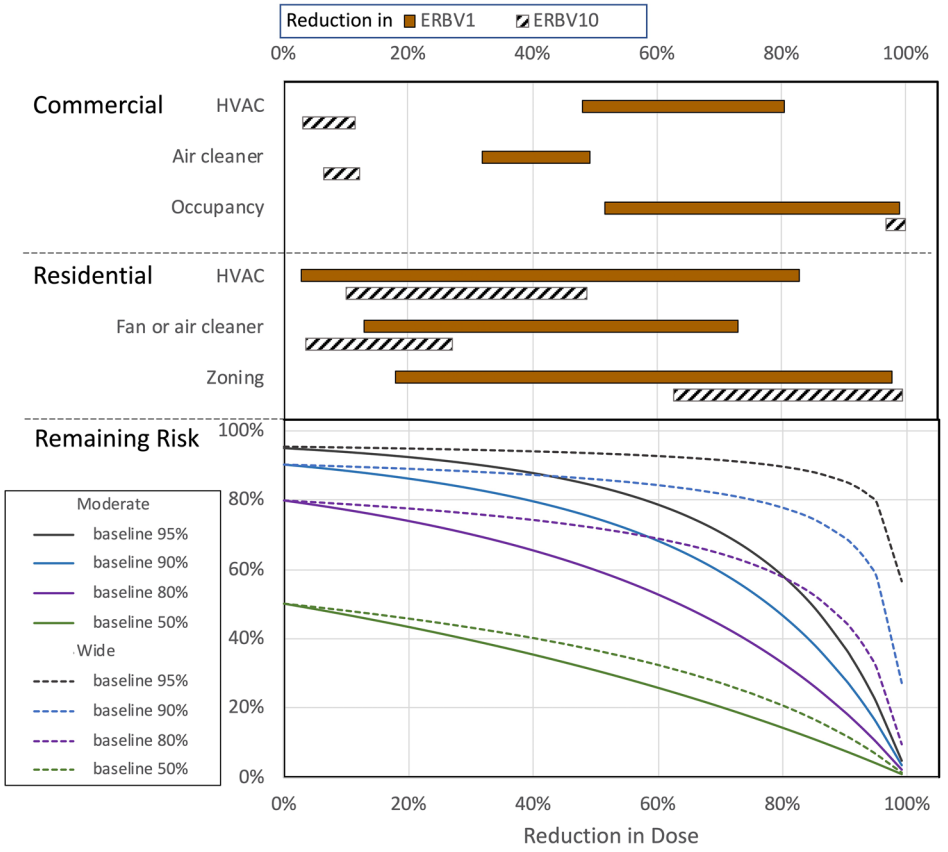

Figure 4. Possible changes in risk associated with reductions in ERBV. Percentage reductions in ERBV (upper *x*-axis) are the same as percentage reductions in dose (lower *x*-axis) and can thus be associated with risk remaining after a specific dose reduction. Baseline risk and dose–response curve width are not known, and uncertainty in risk reduction is demonstrated using illustrative curves with "moderate" and "wide" shapes. Labels on "Office" and "Residential" measures correspond to the specific measures grouped in Figure 3, and ranges for each category cover all measures and situations. $ERBV_{100}$ is not shown because most of the mitigation measures have no effect.

not infect others in the next shift. A similar epidemiological exploitation has been proposed previously.[51]

Mitigation in Meaningful Ranges. Thus far, we have presented ERBV in baseline situations and identified percentage reductions possible with mitigation measures. We now discuss the situations under which those fractional reductions would actually reduce risk.

Figure 4 illustrates risk reductions beginning with four baseline risks and two dose–response curve widths, where the reduction in dose (*x*-axis) corresponds to the change in ERBV. The upper portion of Figure 4 shows the reductions possible from the measures in Figure 3. Risk via $ERBV_1$ is reduced by many mechanical measures in residential situations and most measures in office situations. Except for occupancy strategies, many measures do not have a large effect on risk via $ERBV_{10}$ in office settings. Ventilation strategies do reduce risk via $ERBV_{10}$ in residential settings. When the original risk is very high (95%) and the dose–response curve is wide, the large reductions needed to achieve meaningful reductions are not possible with any mechanical measures.

The dose–response relationship is not known in an emerging disease outbreak. Observations of rebreathed volume can serve as a proxy for dose during early decisions about mitigation. When ERBV is comparable to another situation in which infection has spread widely, mitigation measures that give at least order-of-magnitude reduction should be implemented. Identifying ERBV values when infection does and does not occur could suggest the width of the curve, even if uncertainty in ERBV were a factor of 3 (about $10^{0.5}$).

Practical Uses of Effective Rebreathed Volume. By acknowledging that particle size is the cause of differences in transport, ERBV avoids the legacy "droplet" versus "aerosol" dichotomy. We propose that the following steps would have lessened some of the economic impact associated with the COVID-19 pandemic:

(1) *Building designers* would have determined $ERBV_1$, $ERBV_{10}$, and $ERBV_{100}$ at the time of commissioning, providing values that quantified both normal and transmission-minimizing circumstances.

(2) *Epidemiological studies* would immediately exploit known differences in $ERBV_1$, $ERBV_{10}$, and $ERBV_{100}$ to identify particle sizes associated with infection as soon as outbreaks emerged. They might also identify ERBV associated with saturation and approximate widths of dose–response curves. Effective interventions could then be better targeted.

(3) *Facility managers* could evaluate venues, for example, comparing ERBV for different rooms or for indoor versus outdoor locations. As information emerged, they would be guided in their determination with values of ERBV that were known to be saturated and safe.

(4) *Public health messaging* would include ERBV so that each individual could make informed choices about interactions based on relative and overall risk acceptance.

https://dx.doi.org/10.1021/acs.est.0c07721
Environ. Sci. Technol. 2021, 55, 2890–2898

These types of evaluation have all been conducted casually during the COVID-19 pandemic. We developed the size-dependent ERBV metric to provide rigor to such informal evaluations, to isolate the environmental component of the chain of infection, to identify limiting uncertainties like indoor deposition rates, and to provide a framework that supports rapid response in future outbreaks.

■ ASSOCIATED CONTENT

Supporting Information

The Supporting Information is available free of charge at https://pubs.acs.org/doi/10.1021/acs.est.0c07721.

Supplementary schemes, figures, and tables (PDF)

■ AUTHOR INFORMATION

Corresponding Author

Tami C. Bond − *Mechanical Engineering, Colorado State University, Fort Collins, Colorado 80523, United States;* orcid.org/0000-0001-5968-8928; Phone: (970) 491-4105; Email: tami.bond@colostate.edu

Authors

Angela Bosco-Lauth − *College of Veterinary Medicine and Biomedical Sciences, Colorado State University, Fort Collins, Colorado 80521, United States*

Delphine K. Farmer − *Chemistry, Colorado State University, Fort Collins, Colorado 80523, United States;* orcid.org/0000-0002-6470-9970

Paul W. Francisco − *Energy Institute, Colorado State University, Fort Collins, Colorado 80524, United States; Indoor Climate Research and Training, Applied Research Institute, University of Illinois at Urbana−Champaign, Champaign, Illinois 61820, United States*

Jeffrey R. Pierce − *Atmospheric Sciences, Colorado State University, Fort Collins, Colorado 80523, United States;* orcid.org/0000-0002-4241-838X

Kristen M. Fedak − *Environmental and Radiological Health Science, Colorado State University, Fort Collins, Colorado 80523, United States*

Jay M. Ham − *Soil and Crop Science, Colorado State University, Fort Collins, Colorado 80523, United States*

Shantanu H. Jathar − *Mechanical Engineering, Colorado State University, Fort Collins, Colorado 80523, United States;* orcid.org/0000-0003-4106-2358

Sue VandeWoude − *Microbiology, Immunology, and Pathology, Colorado State University, Fort Collins, Colorado 80523, United States;* orcid.org/0000-0001-9227-1622

Complete contact information is available at: https://pubs.acs.org/10.1021/acs.est.0c07721

Author Contributions

Conceptualization (T.C.B.), methodology (T.C.B., A.B.L., D.K.F., P.W.F., J.R.P., J.M.H.), validation (S.H.J.), cross-disciplinary integration (K.M.F., S.V.), writing, original draft (T.C.B., A.B.L., D.K.F., P.W.F.); writing, review and editing (All).

Notes

The authors declare no competing financial interest.

■ ACKNOWLEDGMENTS

Mj Riches created the artistic rendering of Figure 1. Helpful comments on the manuscript, development, and language came from David Dandy, Greg Hickey, Prasad Kasibhatla, Joshua Keller, Marilee Long, Steven Simske, and Ander Wilson. The author team acknowledges multidisciplinary interactions supported at Colorado State University under initiatives entitled Aerobiome; Partnership for Climate, Air Quality and Health (PACH); and Sustainable Performance of Healthy and Efficient Residential Environments (SPHERE) that have fostered collaborative problem-solving. T.C.B. acknowledges support from Walter Scott, Jr. Presidential Chair funds. D.K.F. was supported by the Alfred P. Sloan Foundation (G-2019-12442).

■ REFERENCES

(1) Makridis, C.; Hartley, J. The Cost of Covid-19: A Rough Estimate of the 2020 US GDP Impact. *Special Edition Policy Brief* **2020**, DOI: 10.2139/ssrn.3570731

(2) Gandhi, M.; Yokoe, D. S.; Havlir, D. V. Asymptomatic Transmission, the Achilles' Heel of Current Strategies to Control Covid-19. *N. Engl. J. Med.* **2020**, *382*, 2158−2160.

(3) He, X.; Lau, E. H. Y.; Wu, P.; Deng, X.; Wang, J.; Hao, X.; Lau, Y. C.; Wong, J. Y.; Guan, Y.; Tan, X. Temporal dynamics in viral shedding and transmissibility of COVID-19. *Nat. Med.* **2020**, *26*, 672−675.

(4) Morse, S. S.; Mazet, J. A. K.; Woolhouse, M.; Parrish, C. R.; Carroll, D.; Karesh, W. B.; Zambrana-Torrelio, C.; Lipkin, W. I.; Daszak, P. Prediction and prevention of the next pandemic zoonosis. *Lancet* **2012**, *380*, 1956−1965.

(5) Dawson, W.; Moser, D.; Van Kleunen, M.; Kreft, H.; Pergl, J.; Pyšek, P.; Weigelt, P.; Winter, M.; Lenzner, B.; Blackburn, T. M. Global hotspots and correlates of alien species richness across taxonomic groups. *Nature Ecology & Evolution* **2017**, *1*, 186.

(6) Keesing, F.; Belden, L. K.; Daszak, P.; Dobson, A.; Harvell, C. D.; Holt, R. D.; Hudson, P.; Jolles, A.; Jones, K. E.; Mitchell, C. E. Impacts of biodiversity on the emergence and transmission of infectious diseases. *Nature* **2010**, *468*, 647−652.

(7) Centers for Disease Control and Prevention. *Principles of epidemiology in public health practice: an introduction to applied epidemiology and biostatistics*, 2006.

(8) Riley, E. C.; Murphy, G.; Riley, R. L. Airborne spread of measles in a suburban elementary school. *Am. J. Epidemiol.* **1978**, *107*, 421−432.

(9) Siegel, J.; Rhinehart, E.; Jackson, M.; Chiarello, L. *Guideline for Isolation Precautions: Preventing Transmission of Infectious Agents in Healthcare Settings (updated July 2019)*, 2007. https://www.cdc.gov/infectioncontrol/guidelines/isolation/index.html.

(10) Tellier, R.; Li, Y.; Cowling, B. J.; Tang, J. W. Recognition of aerosol transmission of infectious agents: a commentary. *BMC Infect. Dis.* **2019**, *19*, 101.

(11) Qian, H.; Miao, T.; Li, L. I. U.; Zheng, X.; Luo, D.; Li, Y. Indoor transmission of SARS-CoV-2. *medRxiv* **2020**, DOI: 10.1101/2020.04.04.20053058.

(12) Chen, W.; Zhang, N.; Wei, J.; Yen, H. L.; Li, Y. Short-range airborne route dominates exposure of respiratory infection during close contact. *Building and Environment* **2020**, *176*, 106859.

(13) Yu, I. T. S.; Li, Y.; Wong, T. W.; Tam, W.; Chan, A. T.; Lee, J. H. W.; Leung, D. Y. C.; Ho, T. Evidence of airborne transmission of the severe acute respiratory syndrome virus. *N. Engl. J. Med.* **2004**, *350*, 1731−1739.

(14) Gralton, J.; Tovey, E.; McLaws, M.-L.; Rawlinson, W. D. The role of particle size in aerosolised pathogen transmission: A review. *J. Infect.* **2011**, *62*, 1−13.

(15) Thomas, R. J. Particle size and pathogenicity in the respiratory tract. *Virulence* **2013**, *4*, 847−858.

(16) Nazaroff, W. W. Inhalation intake fraction of pollutants from episodic indoor emissions. *Building and Environment* **2008**, *43*, 269−277.

(17) Rudnick, S. N.; Milton, D. K. Risk of indoor airborne infection transmission estimated from carbon dioxide concentration. *Indoor air* **2003**, *13*, 237−245.
(18) Zhang, X.; Ji, Z.; Yue, Y.; Liu, H.; Wang, J. Infection Risk Assessment of COVID-19 through Aerosol Transmission: a Case Study of South China Seafood Market. *Environ. Sci. Technol.* **2020**, DOI: 10.1021/acs.est.0c02895.
(19) Buonanno, G.; Morawska, L.; Stabile, L. Quantitative assessment of the risk of airborne transmission of SARS-CoV-2 infection: prospective and retrospective applications. *medRxiv* **2020**, DOI: 10.1016/j.envint.2020.106112.
(20) Miller, S. L.; Nazaroff, W. W.; Jimenez, J. L.; Boerstra, A.; Buonanno, G.; Dancer, S. J.; Kurnitski, J.; Marr, L. C.; Morawska, L.; Noakes, C. Transmission of SARS-CoV-2 by inhalation of respiratory aerosol in the Skagit Valley Chorale superspreading event. *Indoor Air* **2020**, DOI: 10.1111/ina.12751.
(21) Asadi, S.; Wexler, A. S.; Cappa, C. D.; Barreda, S.; Bouvier, N. M.; Ristenpart, W. D. Aerosol emission and superemission during human speech increase with voice loudness. *Sci. Rep.* **2019**, *9*, 1−10.
(22) Johnson, G. R.; Morawska, L.; Ristovski, Z. D.; Hargreaves, M.; Mengersen, K.; Chao, C. Y. H.; Wan, M. P.; Li, Y.; Xie, X.; Katoshevski, D.; Corbett, S. Modality of human expired aerosol size distributions. *J. Aerosol Sci.* **2011**, *42*, 839−851.
(23) Bake, B.; Larsson, P.; Ljungkvist, G.; Ljungström, E.; Olin, A.-C. Exhaled particles and small airways. *Respir. Res.* **2019**, *20*, 8.
(24) Xie, X.; Li, Y.; Chwang, A. T. Y.; Ho, P. L.; Seto, W. H. How far droplets can move in indoor environments − revisiting the Wells evaporation−falling curve. *Indoor Air* **2007**, *17*, 211−225.
(25) Vejerano, E. P.; Marr, L. C. Physico-chemical characteristics of evaporating respiratory fluid droplets. *J. R. Soc., Interface* **2018**, *15*, 20170939.
(26) Humphrey, S. P.; Williamson, R. T. A review of saliva: Normal composition, flow, and function. *J. Prosthet. Dent.* **2001**, *85*, 162−169.
(27) Hanna, S. R.; Briggs, G. A.; Hosker, R. P., Jr. *Handbook on atmospheric diffusion*; National Oceanic and Atmospheric Administration, 1982.
(28) Celani, A.; Villermaux, E.; Vergassola, M. Odor Landscapes in Turbulent Environments. *Phys. Rev. X* **2014**, *4*, 41015.
(29) Farrell, J. A.; Murlis, J.; Long, X.; Li, W.; Cardé, R. T. Filament-based atmospheric dispersion model to achieve short time-scale structure of odor plumes. *Environ. Fluid Mech.* **2002**, *2*, 143−169.
(30) Murlis, J.; Jones, C. D. Fine-scale structure of odour plumes in relation to insect orientation to distant pheromone and other attractant sources. *Physiol. Entomol.* **1981**, *6*, 71−86.
(31) Noakes, C. J.; Sleigh, P. A. Mathematical models for assessing the role of airflow on the risk of airborne infection in hospital wards. *J. R. Soc., Interface* **2009**, *6*, S791−S800.
(32) Ezzati, M.; Saleh, H.; Kammen, D. M. The contributions of emissions and spatial microenvironments to exposure to indoor air pollution from biomass combustion in Kenya. *Environ. Health Perspect.* **2000**, *108*, 833−839.
(33) Drivas, P. J.; Valberg, P. A.; Murphy, B. L.; Wilson, R. Modeling Indoor Air Exposure from Short-Term Point Source Releases. *Indoor Air* **1996**, *6*, 271−277.
(34) Cheng, K.-C.; Acevedo-Bolton, V.; Jiang, R.-T.; Klepeis, N. E.; Ott, W. R.; Fringer, O. B.; Hildemann, L. M. Modeling Exposure Close to Air Pollution Sources in Naturally Ventilated Residences: Association of Turbulent Diffusion Coefficient with Air Change Rate. *Environ. Sci. Technol.* **2011**, *45*, 4016−4022.
(35) ASHRAE. *ANSI/ASHRAE standard 62.2-2019: Ventilation and Acceptable Indoor Air Quality in Residential Buildings*, 2019.
(36) ASHRAE. *ANSI/ASHRAE Standard 62.1-2019: Ventilation for Acceptable Indoor Air Quality*. 2019, Vol. *30329*.
(37) K. Lai, A. C.; Nazaroff, W. W. Modeling Indoor Particle Deposition from Turbulent Flow onto Smooth Surfaces. *J. Aerosol Sci.* **2000**, *31*, 463−476.
(38) Howard-Reed, C.; Wallace, L. A.; Emmerich, S. J. Effect of ventilation systems and air filters on decay rates of particles produced by indoor sources in an occupied townhouse. *Atmos. Environ.* **2003**, *37*, 5295−5306.
(39) Thatcher, T. L.; Layton, D. W. Deposition, resuspension, and penetration of particles within a residence. *Atmos. Environ.* **1995**, *29*, 1487−1497.
(40) Lai, A. C. K. Particle deposition indoors: a review. *Indoor Air* **2002**, *12*, 211−214.
(41) Palmiter, L.; Bond, T. Interaction of mechanical systems and natural infiltration. *Proc. 12th AIVC Conference*, Ottawa, Canada, 1991; pp 285−295.
(42) ASHRAE. *ANSI/ASHRAE standard 52.2−2017: Method of Testing General Ventilation Air-Cleaning Devices for Removal Efficiency by Particle Size*, 2017.
(43) Watanabe, T.; Bartrand, T. A.; Weir, M. H.; Omura, T.; Haas, C. N. Development of a dose-response model for SARS coronavirus. *Risk Analysis: An International Journal* **2010**, *30*, 1129−1138.
(44) Kitajima, M.; Huang, Y.; Watanabe, T.; Katayama, H.; Haas, C. N. Dose−response time modelling for highly pathogenic avian influenza A (H5N1) virus infection. *Lett. Appl. Microbiol.* **2011**, *53*, 438−444.
(45) Miller, S. L.; Nazaroff, W. W. Environmental tobacco smoke particles in multizone indoor environments. *Atmos. Environ.* **2001**, *35*, 2053−2067.
(46) Licina, D.; Tian, Y.; Nazaroff, W. W. Inhalation intake fraction of particulate matter from localized indoor emissions. *Building and Environment* **2017**, *123*, 14−22.
(47) Liu, L.; Li, Y.; Nielsen, P. V.; Wei, J.; Jensen, R. L. Short-range airborne transmission of expiratory droplets between two people. *Indoor Air* **2017**, *27*, 452−462.
(48) Melikov, A. K.; Ai, Z. T.; Markov, D. G. Intermittent occupancy combined with ventilation: An efficient strategy for the reduction of airborne transmission indoors. *Sci. Total Environ.* **2020**, *744*, 140908.
(49) Ai, Z. T.; Melikov, A. K. Airborne spread of expiratory droplet nuclei between the occupants of indoor environments: A review. *Indoor Air* **2018**, *28*, 500−524.
(50) Keating, B. A.; Thorburn, P. J. Modelling crops and cropping systems—Evolving purpose, practice and prospects. *Eur. J. Agron.* **2018**, *100*, 163.
(51) Stilianakis, N. I.; Drossinos, Y. Dynamics of infectious disease transmission by inhalable respiratory droplets. *J. R. Soc., Interface* **2010**, *7*, 1355−1366.